

# TOY MODELS OF NON-PERTURBATIVE ASYMPTOTIC FREEDOM IN $\phi_6^3$

J.M. Cornwall\* and D.A. Morris†

*Physics Department, University of California at Los Angeles*

*405 Hilgard Ave., Los Angeles, CA 90095-1547*

## Abstract

We study idealizations of the full nonlinear Schwinger-Dyson equations for the asymptotically free theory of  $\phi^3$  in six dimensions in its meta-stable vacuum. We begin with the cubic nonlinearity and go on to all-order nonlinearities which contain instanton effects. In an asymptotically free theory the relevant Schwinger-Dyson equations are homogeneous and ultraviolet finite and perturbative methods fail from the outset. We show how our toy models of the cubic Schwinger-Dyson equations contain the usual diseases of perturbation theory in the massless limit (e.g., factorially-divergent  $\beta$ -functions, singular Borel-transform kernels associated with infrared renormalons) and show how these models yield specific mechanisms for removing such singularities when there is a mass gap. The solutions to these homogeneous equations, in spite of being ultraviolet finite, still depend on an undetermined parameter equivalent to the perturbative renormalization scale  $\mu$ . In the all-order nonlinear equation we show how to recover the usual renormalization-group-improved instanton effects and associated factorial divergences.

UCLA/95/TEP/20

June 1995

---

\*Electronic address: cornwall@physics.ucla.edu

†Electronic address: dmorris@physics.ucla.edu

## I. INTRODUCTION

Asymptotically free theories appear to have perturbatively calculable properties in the ultraviolet (UV) where the running coupling gets small. The well-known price paid for this convenience of perturbation theory in the UV is its complete breakdown at some low momentum scale, usually thought of as being of  $O(\Lambda_{\text{RG}})$  where  $\Lambda_{\text{RG}}$  is the renormalization group (RG) mass. However, as one goes to higher orders  $N$  in perturbation theory, the critical momentum scale grows exponentially in  $N$  essentially because the number of graphs grows as  $N!$ . That is to say, the contribution of the  $N^{\text{th}}$  order term in perturbation theory behaves like  $N!(a\bar{g}^2)^N$  where  $\bar{g} \sim (\ln k^2)^{-1/2}$  is the running charge; to keep this term small as  $N$  grows requires an exponential increase in  $k^2$ . There are also factorial divergences associated with renormalons [1]. Consequently, perturbation theory to all orders cannot be used for any momentum scale, however large, in an asymptotically free theory without understanding how to deal with non-Borel-summable factorial divergences. This is currently not a practical limit on perturbation theory in QCD, where the critical momentum does not creep into the UV until  $N$  is rather large, say  $N \geq 10$ .

A more practical issue is understanding QCD processes at infrared (IR) scales  $k \sim \Lambda_{\text{RG}}$  and the attendant phenomena of confinement, condensates, renormalons, large instantons, etc. [2] The purpose of the present paper is to discuss the factorial divergences mentioned above, as well as IR issues (except for confinement) in a toy model of asymptotic freedom [3]:  $\phi^3$  in six dimensions ( $\phi_6^3$ ). This theory is terminally ill because the Hamiltonian is unbounded below but we can go quite far before encountering pathologies. The idea is to study the theory at all momentum scales from the IR to the UV in a connected way, without using the conventional crutches of perturbation theory. Our study will use the machinery of nonlinear Schwinger-Dyson equations [4] for  $\phi_6^3$ .

Even without the spin complications of QCD, it is too hard for us to solve the full Schwinger-Dyson equations numerically, even if only the cubic nonlinearity is saved in the Schwinger-Dyson equation for the vertex. So we turn to toy models, first saving only the cubic term for the vertex and later considering some aspects of the all-order nonlinearities in the vertex equation. Although we have no proof, we believe that these toy models fairly represent qualitatively, but not quantitatively, all the diseases and their cures we would encounter in the full Schwinger-Dyson

equations.

Of course, any study of  $\phi_6^3$  must ultimately break down because the theory itself is ill-defined; it has no stable vacuum. We will see that the breakdown occurs when we try to define the sum of the non-Borel-summable  $N!$  divergences associated with vertex skeleton graphs having  $2N+1$  vertices. These sums contain the contributions of instantons [5,6], which we need not add as an explicit ingredient in analyzing the field theory; they are already in the Schwinger-Dyson equations.

The Schwinger-Dyson equations of an asymptotically free theory have a special feature: the renormalization constants which appear in the renormalized Schwinger-Dyson equations must vanish. This vanishing is clear from the canonical form of the  $\phi_6^3$  vertex equation (or its analog in QCD), in which the vertex renormalization constant  $Z_1$  appears only as an additive inhomogeneous term. At large momentum, asymptotic freedom requires the vertex and all the other terms of the Schwinger-Dyson equation to vanish, as we will show; this is inconsistent unless  $Z_1 = 0$ . However, one must be careful. The unqualified statement  $Z_1 = 0$  is false and leads to paradoxes. A more precise statement resembles that of lattice gauge theory where the theory is first defined with an UV cutoff  $\Lambda_{UV}$  and  $Z_1 \rightarrow 0$  at a specific rate as  $\Lambda_{UV} \rightarrow \infty$ .

We will see that it is correct simply to set  $Z_1 = 0$  in the canonical form of the vertex equation (or in an analogous equation for the running coupling, which is RG-invariant). The resulting vertex equation is homogeneous, which completely disconnects it from any perturbative approach and vastly complicates the analysis in some ways.

At this point we turn to toy models of the homogeneous and nonlinear vertex Schwinger-Dyson equation. Not all models that we have studied will be presented, since they all show the same features. We believe that all these features will occur in the full Schwinger-Dyson equation as well. Our studies (both analytic and numeric) fall into several categories:

*1A-Cubic nonlinearity: massless.* The toy-model vertex Schwinger-Dyson equation for the running coupling can be converted to a (nonlinear) ordinary differential equation. There are several types of solutions, all of them having singularities at sufficiently small momenta and having undetermined parameters. One of them behaves as expected from perturbation theory for large momentum where the running coupling varies as  $(\ln k^2)^{-1/2}$ ; other solutions vanish as an inverse

power of  $k^2$  (modulo logarithms). We find a differential equation for the  $\beta$ -function whose power-series solution diverges like  $N!$ , with all terms negative [4]; this divergence is associated with IR renormalons. We use the Laplace transform of the vertex equation in  $\ln k^2$  to find an equation for the Borel transform of, e.g., the  $\beta$ -function, and find explicitly its pole structure at the IR renormalon singularity.

*1B-Cubic nonlinearity: massive.* In this case, as is well-known, all the IR renormalon difficulties are resolved (at least for large enough mass), and the toy-model Schwinger-Dyson equations are non-singular. The only solutions which are regular for all Euclidean momenta behave like  $(\ln k^2)^{-1/2}$  for large  $k$ . All solutions depend on a single continuous real parameter, equivalent to the RG renormalization point  $\mu$ ; this is somewhat of a surprise, since all models yield UV-finite solutions needing no cutoff or other regularization. Modulo this parameter, the solutions show uniquely-determined power-law corrections to perturbation theory (e.g., condensates and other higher-twist terms). Generally, the toy models (as well as the full Schwinger-Dyson equation) cannot be reduced to differential equations, but there is one notable exception, which we analyze in some detail. As for the massless case, this is a cubically-nonlinear second-order ordinary differential equation. The Laplace-transform form of the vertex equation shows that the renormalon pole singularity is cancelled by another term vanishing like an inverse power of  $k^2$  (modulo logarithms) at large  $k$ .

*2. All-order nonlinearity.* First, we prove a theorem (similar to another used recently [7] to study  $N!$  divergences in  $\phi_4^4$ ) that the imaginary part, in Minkowski space, of every skeleton graph for the  $\phi_6^3$  vertex has neither IR nor UV logarithms. The implication is that the UV and IR behavior of the dressed graphs is entirely determined by the dressed vertex itself, which allows for an approach to the all-order problem by successive approximations, beginning by inputting the solutions to the cubic Schwinger-Dyson equation. When we use the  $(\ln k^2)^{-1/2}$  behavior found earlier as input, we find that the  $N$ -vertex graph has the asymptotic UV behavior  $\sim (\ln k^2)^{-(N-2)/2}$ . Using some deep graph-theoretic results and other tools developed in an earlier  $\phi_4^4$  study, we show that this momentum factor is multiplied by  $a^N N!$ , where the positive constant  $a$  is rather close to what would be expected from a one-loop RG-improved instanton analysis. The sum over all

$N$  is ambiguous, but should have an imaginary part reflecting the instability of  $\phi_6^3$ . The real part shows the usual power-law behavior expected from instantons.

We comment on some of these results in more detail. Among our major results are our demonstrations of i) how the Schwinger-Dyson equation can be expressed as a nonlinear integral equation for what would be called the Borel transform in perturbation theory, ii) how the massless Schwinger-Dyson equation gives rise to poles in this transform and iii) how the massive Schwinger-Dyson equation gets rid of these poles by condensate terms. In its simplest terms, the massless case yields a Borel integral for the  $\beta$ -function derived from the running coupling of the form

$$\beta(g) = \text{constant} \times \int_0^\infty d\alpha \frac{H(\alpha)}{2-\alpha} e^{-\alpha/(bg^2)} \quad (1)$$

where  $H(\alpha)$  is regular at  $\alpha = 2$ . This corresponds to a  $\beta$ -function with terms behaving like  $-g^{2N+1}(b/2)^N N!$  at large  $N$ . Here  $b$  is the lowest-order coefficient in the  $\beta$ -function:  $\beta = -bg^3 + \dots$ .

We show that, when masses are included, Eq. 1 changes to

$$\beta(g) = \text{constant} \times \int_0^\infty d\alpha \frac{H(\alpha)}{2-\alpha} \left( e^{-\alpha/(bg^2)} - e^{-2/(bg^2)} \right) \quad (2)$$

which has no singularity at  $\alpha = 2$ . The running coupling has a similar expression, but with  $1/(bg^2)$  replaced by  $\ln(k^2 + M^2)$ ; this shows that the cancellation involves terms vanishing like  $(k^2)^{-2}$  at large  $k$ . Of course, the perturbative expansion of the  $\beta$ -function is the same as before, but Eq. 2 shows how that sum is actually defined by the Schwinger-Dyson equation.

Another interesting result is that all our toy models, while perfectly finite in the UV and requiring no cutoffs or regularizations, still have a single real parameter in the solutions, which is not fixed by the vertex Schwinger-Dyson equation above. This parameter is equivalent to the usual renormalization-point mass  $\mu$  of perturbation theory, which arises precisely because perturbation theory requires a cutoff. We believe that this parameter persists even in the homogeneous, finite Schwinger-Dyson equation because, as mentioned above, the categorical statement  $Z_1 = 0$  is not true. There are other forms of the vertex Schwinger-Dyson equation in which it is essential to introduce a cutoff and cancel the cutoff dependence of  $Z_1$  against that of various integrals involving the vertex. In other words, the homogeneous finite Schwinger-Dyson equation we use recognizes its heritage as a renormalizable, not super-renormalizable, theory. It is, of course, possible that

combining the study of the Schwinger-Dyson vertex with some other Schwinger-Dyson equation of the theory would fix the free parameter we find, but we have no evidence for that.

A final result worth commenting on is the partial uncovering of instanton phenomena in sums of graphs—not just bare graphs, but dressed graphs, which leads to the incorporation of what would be called one-loop RG effects at our level of investigation. It is not straightforward to deal with instantons in the usual way, improving semi-classical results with the perturbative RG. For one thing, these perturbative corrections to instantons are not under control any more than they are in other sectors of the theory; there are IR renormalons which must be tamed by masses as in Eq. 2. Furthermore, there are no exact instantons in the massive theory and perhaps most crucial, standard instanton techniques are really only applicable when all external momenta vanish [8]. Ultimately, instanton effects at all momentum scales will have to be dealt with by Schwinger-Dyson methods. What we leave completely open here is how unitarity or some other physical effect provides a definition for the divergent sums associated with instantons. One would not be surprised to find a modification like Eq. 2 entering for instantons as well as IR renormalons, at least in a well-behaved theory like QCD.

Which of our results might persist in the theory of real interest to us, QCD? Even forgetting about confinement, the major complication which sets QCD apart from  $\phi_6^3$  is gauge invariance. Using the pinch technique [4,9], however, it is possible to define gauge-invariant proper vertices and self-energies which are related by naive (ghost-free) Ward identities. For these special vertices and self-energies  $Z_1 = Z_2$ , and both these renormalization constants vanish like  $(\ln \Lambda_{UV}^2)^{-1/2}$  as  $\Lambda_{UV} \rightarrow \infty$ ; one can, in principle at least, write down finite homogeneous Schwinger-Dyson equations for the gauge-invariant vertex corresponding to the running coupling, and these should show phenomena similar to what we did for  $\phi_6^3$ . For example, generation of a QCD mass scale is expected to yield a renormalon cancellation mechanism like that expressed in Eq. 2 for Borel-transform renormalon poles; indeed, this mechanism has already been invoked [10] on other grounds. It is also reasonable to expect that we can find instanton phenomena in graphical sums, just as for  $\phi_6^3$ .

As for persistence of a free parameter like  $\mu$ , the situation is not so clear. The vertex and propagator are not independent as they are in  $\phi_6^3$ , which might lead to further constraints. One

expects that QCD (without quarks) has only one free parameter, the RG mass  $\Lambda_{\text{RG}}$ , in terms of which all physical quantities are determined. This does not seem to be the case for  $\phi_6^3$ , which has both  $\mu$  and the mass  $M$  free, at least at the level of our investigation.

## II. PRELIMINARIES

In this section we make some general remarks about the nature of the perturbation series for  $g\phi^3$  theories. We encounter non-Borel-summable series in  $g$  of the usual asymptotically free type, but in certain cases these series define one or more entire functions of  $g$ . We also set the stage for the investigation of  $\phi_6^3$ , discussing some aspects of the Schwinger-Dyson equations for the proper vertex, the proper self-energy, and a vertex formed from these which is RG invariant and corresponds to the running charge.

### A. General $\phi^3$ Theories

Theories of  $\phi^3$  type are well-defined, in general, only for purely imaginary coupling where they sometimes make sense physically [11,12]. It is sometimes possible to continue the theory to real  $g$  by imposing definitions (typically, the order in which integrals are to be done) which may or may not make sense physically. Consider as an example a zero-dimensional model with two fields  $x$  and  $y$  with a partition function given by

$$Z(g) = \int_{-\infty}^{\infty} dx dy e^{-x^2 - y^2 + gx^2 y} \quad (3)$$

which is well-defined if  $g$  is imaginary. We can give two forms to  $Z$  depending on which order the integrals are done; integrating over  $y$  first gives

$$Z(g) = \sqrt{\pi} \int_{-\infty}^{\infty} dx e^{-x^2 + g^2 x^4 / 4} \quad (4)$$

which is a wrong-sign  $\phi^4$  theory. Expanding Eq. 4 in powers of  $g^2$  gives rise to a typical asymptotically free series with terms behaving like  $N! N^b (ag^2)^N$  where  $a$  and  $b$  are fixed constants with  $a > 0$ . It is not obvious how such a divergent series is to be defined.

If we instead perform the integral over  $x$  first in Eq. 4 we get

$$Z(g) = \sqrt{\pi} \int_{-\infty}^{\infty} dy (1 - gy)^{-1/2} e^{-y^2} . \quad (5)$$

This appears to be singular at  $y = 1/g$  (the classical saddle point) of Eq. 3 but in fact  $Z(g)$  as defined by Eq. 5 is an entire function of  $g$ : as  $g$  changes from a pure imaginary value to the real axis, or anywhere else in the complex  $g$ -plane, the contour can be deformed to avoid the potential singularity. Actually, Eq. 5 defines two entire functions, depending on whether one begins with  $g$  on the positive or negative imaginary axis. One or the other of these possibilities may be singled out by physical considerations, or a linear combination may be used (e.g., the average of the two entire functions is real for real  $g$ ).

These remarks can be generalized to  $d = 6$  theories of the type  $g\phi|\psi|^2$  where  $\phi$  is a single-component Hermitian field, and  $\psi$  is a single-component complex field. The Euclidean partition function is

$$Z = \int (d\phi d\bar{\psi} d\psi) \exp \left[ - \int d^6x \left( |\partial_\mu \psi|^2 + \frac{1}{2} (\partial_\mu \phi)^2 + g\phi|\psi|^2 + \text{mass terms} \right) \right] . \quad (6)$$

The functional integral over  $\phi$  is free, and when done reveals a wrong-sign non-local  $|\psi|^4$  theory for  $\psi$ , analogous to Eq. 5. But doing the (free-field) functional integral over  $\psi$  gives

$$Z \sim \int (d\phi) \exp \left[ - \int d^6x \left( \frac{1}{2} (\partial_\mu \phi)^2 + \frac{1}{2} M^2 \phi^2 - \text{Tr} \ln(-\square + m^2 + g\phi) \right) \right] . \quad (7)$$

Superficially this would appear to define an entire function of  $g$ , since the quadratic terms in the action dominate the logarithm. However, the argument of the logarithm may vanish (when  $\phi \sim M^2/g$ ) and no firm conclusion can be drawn. Moreover, dimensional transmutation tells us that  $g$  must disappear, to be replaced by a running coupling. Still, it is intriguing to speculate that asymptotically free theories in general may have matrix elements and Green's functions which are entire functions of the running charge. If some such speculation is correct, it can only be developed by methods completely divorced from perturbation theory.

## B. The Schwinger-Dyson Equations for $\phi_6^3$

Throughout this paper (except for section IV) we work only at Euclidean momenta; the action for our theory is

$$S = \int d^6x \left[ \frac{1}{2} (\partial_\mu \phi)^2 + \frac{M^2}{2} \phi^2 + \frac{g}{3!} \phi^6 \right]. \quad (8)$$

We initially focus our attention on the Schwinger-Dyson equations for the renormalized propagator  $\Delta$  and proper vertex  $\Gamma$ . Later we will construct the running coupling from a particular combination of these quantities. The equation for  $\Gamma$  can be written in several equivalent ways. In Fig. 1 we express  $\Gamma$  in terms of a four-point function which is two-particle-irreducible in the  $k_1$  channel. The four-point function can then be decomposed in terms of skeleton graphs and three-point functions. In this and other figures, a small blob denotes  $\Gamma$ , a line denotes  $\Delta$  (both of which are renormalized quantities) and  $Z_1$  is the vertex renormalization constant. Figure 2 shows the analogous equations for  $\Gamma$  in terms of the one-particle-irreducible four-point function and Fig. 3 shows the equation for the inverse propagator.

One of our major concerns will be that  $Z_1$  vanishes in an asymptotically free theory. This is not entirely an elementary matter since uncritically setting  $Z_1 = 0$  in Fig. 2 or the first equation for  $\Delta^{-1}$  in Fig. 3 appears to give zero. The resolution, of course, is that the theory is defined first with an ultraviolet cutoff  $\Lambda_{UV}$  which renders  $Z_1$  finite. In reality, as  $\Lambda_{UV} \rightarrow \infty$  the product of  $Z_1$  with a quantity involving a single bare vertex actually remains finite since the  $\Lambda_{UV}$  dependence of such quantities cancels that of  $Z_1$ . It is permitted, however, to set  $Z_1 = 0$  in those forms of the Schwinger-Dyson equations in which no bare vertex appears (e.g., for  $\Gamma$  in Fig. 1 and the second form for  $\Delta^{-1}$  in Fig. 3). The reason is that in an asymptotically free theory the remaining dressed graphs of the Schwinger-Dyson equation are all individually finite. This does not mean that the Schwinger-Dyson equations are unambiguously finite, since the Schwinger-Dyson equation for  $\Gamma$ , expressed in terms of  $\Gamma$  and  $\Delta$ , has infinitely many terms and the sum actually diverges, as we discuss in Section IV.

Let us concentrate for the moment on the lowest-order Schwinger-Dyson equations for  $\Gamma$  and  $\Delta^{-1}$ , shown in Fig. 4, where we have now set  $Z_1 = 0$ . Introduce the notation

$$\Delta^{-1}(k^2) = (k^2 + M^2)Z_2(k^2) \quad (9)$$

where  $M^2$  is the renormalized mass. We anticipate, guided by one-loop RG-improved perturbation theory [3], that the solutions to the Schwinger-Dyson equations of Fig. 4 behave in the UV ( $k^2 \gg$

$M^2$ ) as various powers of a logarithmic function  $D(k^2)$ :

$$D(k^2) = 1 + bg^2 \ln(k^2/M^2) \quad (10)$$

$$\Gamma \rightarrow D^{-\alpha}, \quad Z_2 \rightarrow D^{-\gamma} . \quad (11)$$

In Eq. 10,  $b$  is a positive number given below; it is the same coefficient as in the one-loop  $\beta$ -function  $\beta = -bg^3 + \dots$ . Any finite mass may be used to set the argument of the logarithm in Eq. 10 and in consequence the 1 on the right hand side of this equation is irrelevant; we will drop it.

Insert these forms into the equation for  $\Gamma$  of Fig. 4a using a simplified form suitable for finding the UV behavior:

$$\Gamma(k^2) = \frac{\pi^3 g^2}{2(2\pi)^6} \int_{k^2}^{\infty} \frac{dp^2}{p^2} (bg^2 \ln p^2)^{3\gamma-3\alpha} = (bg^2 \ln k^2)^{-\alpha} . \quad (12)$$

Doing the integral reveals consistency, provided that

$$1 - 2\alpha + 3\gamma = 0, \quad (13)$$

$$2(4\pi)^3 \alpha b = 1 . \quad (14)$$

Note that if the condition of Eq. 13 is satisfied,  $g^2$  drops out of the equation so we might as well drop it in  $D$  of Eq. 10, along with the 1 previously dropped. That is, there really is no coupling constant in an asymptotically free theory, only mass scales.

We need one more equation to determine  $\alpha, \gamma$ , and  $b$ , which is furnished by the  $\Delta^{-1}$  equation. This is slightly ticklish because it has a quadratic divergence, subsumed by mass renormalization. In a  $g\phi|\psi|^2$  theory one may avoid direct consideration of the  $\Delta^{-1}$  equation by coupling  $\psi$  to the electromagnetic field in the usual way, computing the lowest-order electromagnetic vertex shown in Fig. 5, using the Ward identity

$$q^\mu \Gamma_\mu^{(\gamma)}(q, p, p') = \Delta^{-1}(p) - \Delta^{-1}(p') \quad (15)$$

and then setting  $p'^2 = M^2$ , so  $\Delta^{-1}(p'^2) = 0$ . It turns out (see below) that  $Z_2 = 0$  also, so the  $\Gamma^{(\gamma)}$  equation is homogeneous of Baker-Johnson-Willey type. We leave it to the reader to conduct an analysis like that which led to Eq. 12; it gives the same result as Eq. 16 below.

Either as sketched above or by analysis of the  $\Delta^{-1}$  equation in Fig. 3 one finds a new condition

$$(4\pi)^3 \gamma b = 1/12 . \quad (16)$$

Then one finds

$$\alpha = 2/3 , \quad \gamma = 1/9 , \quad b = \frac{3}{4(4\pi)^3} \quad (17)$$

which are the usual results [3] of one-loop RG-improved perturbation theory, with  $\beta$ -function  $-bg^3 + \dots$ . These constants also appear in the cutoff dependence of the perturbative renormalization constants

$$Z_1 = \left(1 + bg^2 \ln(\Lambda_{\text{UV}}^2/\mu^2)\right)^{-2/3}, \quad Z_2 = \left(1 + bg^2 \ln(\Lambda_{\text{UV}}^2/\mu^2)\right)^{-1/9} \quad (18)$$

both of which vanish as the cutoff  $\Lambda_{\text{UV}} \rightarrow \infty$ .

At this point it is convenient to introduce a special combination of  $\Gamma$  and  $Z_2$ , corresponding to the running charge

$$\bar{g}(k_1, k_2, k_3) \equiv g \frac{\Gamma(k_1, k_2, k_3)}{\sqrt{Z_2(k_1)Z_2(k_2)Z_2(k_3)}} . \quad (19)$$

We keep the explicit  $g$  only to observe that, with  $D \equiv bg^2 \ln k^2$ ,  $\Gamma \sim D^{-2/3}$ ,  $Z_2 \sim D^{-1/9}$ , all the  $g$ 's cancel in Eq. 19. We now find the asymptotic behavior, when all  $k_i$  scale like a large momentum  $k$ ,

$$\bar{g}^2 \rightarrow \frac{1}{b \ln k^2} . \quad (20)$$

This is the usual one-loop running coupling. If constructed in perturbation theory,  $\bar{g}$  would be explicitly independent of the renormalization point  $\mu$ .

With  $Z_1 = 0$ , the Schwinger-Dyson equation for  $\bar{g}$  (the solid blob in Fig. 6) looks like that for  $\Gamma$  with the important difference that now the propagator lines correspond to free propagators with the renormalized mass. This seems to lead to a quite remarkable circumstance in which the Schwinger-Dyson equation for  $\bar{g}$  is completely self-contained. However, this is misleading since the infinite series of terms in Fig. 6 does not have a sum which is well-defined. In fact, this series contains the basic instanton phenomenon of  $\phi_6^3$ , as we will see in Section IV, but we will never need to invoke instantons explicitly. We will also see in Section IV that Schwinger-Dyson graphs

for  $\bar{g}$  having  $2N + 1$  insertions of  $\bar{g}$  behave at large momentum like  $(\ln k^2)^{-N/2}$ , so that the leading UV behavior is correctly captured in the cubic graph.

In the next section we will investigate toy models of the Schwinger-Dyson equation somewhat similar to the integral of Eq. 12. If we uncritically write such an equation for  $\bar{g}$  with free propagators ( $\gamma = 0$ ) and test whether  $\bar{g} = (b \ln k^2)^{-1/2}$  is a solution, we find that everything works except that the integral is  $4/3$  larger than it should be. This is because the simple form assumed for  $\bar{g}$  does not distinguish the momenta on the legs of  $\bar{g}$  which are in general different; this distinction matters for  $\bar{g}$  with its separate powers of  $Z_2(k_i)^{-1/2}$ , not all of which involve momenta which are integrated over. In the toy models of the next section we will compensate for this by multiplying the right hand side of integrals cubic in  $\bar{g}$  by  $3/4$ .

Why do we need toy models at all? The answer is that even without the spin complications of QCD, and saving only cubic nonlinearities, the full Schwinger-Dyson equation for  $\phi_6^3$  is quite complicated. Here we set up this cubic equation schematically, before going on to the toy models in the next section.

The proper vertex  $\Gamma(k_1, k_2, k_3)$  depends on three scalar variables  $k_1^2, k_2^2, k_3^2$  in a way which is constrained by causality and spectrum conditions. These may be enforced with the Nakanishi representation [13], which is derived from the Feynman-parameter representation of graphs but which is expected to hold even for non-perturbative processes. For the vertex it reads:

$$\Gamma(k_1, k_2, k_3) = \int dz_1 dz_2 dz_3 d\sigma \delta(1 - z_1 - z_2 - z_3) \frac{h(\sigma, z_1, z_2, z_3)}{\sigma + z_1 k_1^2 + z_2 k_2^2 + z_3 k_3^2}. \quad (21)$$

The spectrum is expressed through the support of  $h$ . In a massive theory, the lower limit of the  $\sigma$  integral depends on masses and  $z_i$  whereas the upper limit is infinity. The asymptotic behavior  $\Gamma \sim (\ln k^2)^{-2/3}$  requires that  $h \sim (\ln \sigma)^{-5/3}$  at large  $\sigma$  (in perturbation theory  $h \rightarrow \text{constant}$ , and Eq. 21 needs the usual subtraction). One then uses Eq. 21 and the Lehmann representation for the propagator to write out the Schwinger-Dyson equation of Fig. 6. If the loop momentum is called  $p$ , the momentum integral depends on three scalars  $(p^2, p \cdot k_1, p \cdot k_2)$ . One might then try to solve the equations numerically, but it is a substantial project. If each  $k_i^2$  takes on 100 values, one has to do  $10^6$  three-dimensional integrals numerically for every iteration. We have not attempted this, but have studied some toy models which we are convinced have the qualitative features as

the real (cubic) Schwinger-Dyson equation. We now turn to those models.

### III. THE TOY MODELS

We have examined several models based on simplifying the cubic Schwinger-Dyson equation of Fig. 1; we will describe a few here. A simplification common to all the models is to assume that  $\Gamma(k_1, k_2, k_3)$  depends only on  $k_1^2 + k_2^2 + k_3^2$  which corresponds to fixing all  $z_i = 1/3$  in the Nakanishi representation of Eq. 21.

In this section we restrict ourselves to the special momentum configuration  $k_1 = 0, k_2 = -k_3 = k$ , and we will be interested in the whole (Euclidean) range  $0 \leq k^2 \leq \infty$ . We will always use free propagators in the model Schwinger-Dyson equation, which can either be interpreted as an approximation to the propagators in the Schwinger-Dyson equation for the proper vertex  $\Gamma$ , or as a special kind of simplification of the Schwinger-Dyson equation for the running coupling  $\bar{g}$ , where free propagators are required (see the discussion around Eq. 19), but where the assumption of dependence of  $\bar{g}$  only on  $\sum k_i^2$  cannot really be correct because of the  $(Z_2(k_1)Z_2(k_2)Z_2(k_3))^{-1/2}$  factor in its definition in Eq. 19. We choose to present our results as referring to  $\bar{g}$ ; the error committed in assuming  $\bar{g}$  depends only on  $\sum k_i^2$  is quantitative but does not affect our major qualitative conclusions. The reason for our choice of interpretation is that all model solutions behave like  $\bar{g}$  in the UV region, that is, like  $(\ln k^2)^{-1/2}$ .

Various models differ from each other by further simplification of the momenta appearing in internal vertices. The Schwinger-Dyson equation with correct momentum assignments is shown in Fig. 7, and corresponds to the integral equation

$$G(2k^2) = \int \frac{d^6 p}{\pi^3} \frac{G(2(p+k)^2)G^2(p^2 + k^2 + (p+k)^2)}{((p+k)^2 + m^2)^2 (p^2 + M^2)}. \quad (22)$$

where the normalization is chosen so that  $G \rightarrow (\ln k^2)^{-1/2}$  for  $k^2 \gg M^2, m^2$  so that we interpret  $G$  as  $b^{1/2}\bar{g}$ . Later we will present numerical solutions of Eq. 22, but for now it is much more important to have an analytic understanding of simplified versions of this equation. The reason for using two masses  $M$  and  $m$  will be made clear later.

### A. The Massless Model.

The first model to be considered is the massless model ( $M = m = 0$ ) where, to make things more tractable, we set  $k = 0$  in the arguments of  $G$  on the right hand side of Eq. 22 to get

$$G(2k^2) = \int \frac{d^6 p}{\pi^3} \frac{G^3(2p^2)}{(p+k)^4 p^2}. \quad (23)$$

It can be shown, by an uninteresting argument bounding  $G$  from above and below, that the solutions to Eq. 22 and Eq. 23 have the same behavior for large  $k$ .

Performing the angular integrals in Eq. 23 and introducing the variables

$$t = \ln(k^2/\mu^2) \quad t' = \ln(p^2/\mu^2) \quad (24)$$

where  $\mu$  is an arbitrary mass scale, we obtain the one-dimensional integral equation

$$G(t) = \frac{1}{2} \int_{-\infty}^{\infty} dt' G^3(t') + \frac{1}{2} \int_{-\infty}^t dt' e^{2(t-t')} G^3(t'). \quad (25)$$

Differentiating twice, one finds that  $G$  obeys the equation

$$\ddot{G} + 2\dot{G} = -G^3 \quad (26)$$

where  $\dot{G} \equiv dG/dt$ . This same equation could be obtained by noting in Eq. 23 that  $[-4\pi^3(p+k)^4]^{-1}$  is the inverse of the d'Alembertian operator in six dimensions.

We must point out that Eq. 26 actually makes no sense if we require  $G(t) \geq 0$  (as physical considerations suggest). Perhaps the most intuitive way to see this is to think of Eq. 26 as the differential equation governing the ‘position’  $G$  of an anharmonic oscillator as a function of ‘time’  $t$ : except for the trivial solution ( $G = 0$ ) all solutions to this equation inevitably develop unbounded oscillations as  $t \rightarrow -\infty$ . The problematic region  $t \rightarrow -\infty$  corresponds to an IR divergence at  $k = 0$ . It is this divergence which is responsible for the renormalon behavior we will shortly encounter. The  $t \rightarrow +\infty$  solutions are candidates for the large- $k$  behavior for the massive equation of Eq. 22.

There are at least two fundamental types of large- $t$  solutions to Eq. 26, and another which is a hybrid of the first two. In the first type, the  $\ddot{G}$  term in Eq. 26 is treated as a perturbation to the equation  $2\dot{G} = -G^3$  which has a solution  $G = t^{-1/2} = (\ln(k^2/\mu^2))^{-1/2}$ , as anticipated from

field-theoretic perturbation theory. Including the  $\ddot{G}$  term as a perturbation, we exhibit several more terms of this solution,

$$G = D^{-1/2} ; \quad D = t + \frac{3}{4} \ln c_1 t - \frac{15}{8t} \left( 1 - \frac{3}{10} \ln c_2 t \right) + \dots . \quad (27)$$

Here the  $c_i$  are constants not determined by consideration of large  $t$  alone.

The behavior of Eq. 27 is, except for the numerical coefficients, precisely what the RG and perturbation theory would give for the running coupling. In fact, it is possible to find the  $\beta$ -function for the vertex  $\bar{g}$  by noting that

$$\beta(\bar{g}) = 2\bar{g} = 2b^{-1/2}\dot{G} \quad (28)$$

which leads immediately from Eq. 26 to a first-order differential equation for  $\beta(g)$ :

$$\beta \left( 1 + \frac{1}{4} \frac{d\beta}{dg} \right) = -bg^3 . \quad (29)$$

The power series solution beginning with  $bg^3$  shows a non-Borel-summable factorial divergence associated with renormalons,

$$\beta(g) \doteq - \sum N! \left( \frac{b}{2} \right)^N g^{2N+1} . \quad (30)$$

where, for large  $N$ ,  $\doteq$  means equality up to fixed powers of  $N$  and overall multiplicative constants. We will return to this solution and the associated  $\bar{g}$  shortly, showing how to set up Eq. 26 directly as an integral equation for a Borel transform.

There is another class of solutions to Eq. 26 which shows no relation to perturbation theory; this class arises from by treating the  $-G^3$  term in Eq. 26 as a perturbation. The solution reads

$$G = \frac{A e^{-2t}}{D_1}; \quad D_1 = 1 + \frac{A^2}{24} e^{-4t} + \frac{A^4}{5760} e^{-8t} + \frac{A^6}{967680} e^{-12t} + \dots . \quad (31)$$

where  $A$  is an arbitrary positive constant. Note that this solution behaves as inverse powers of  $k^4$ , powers which one would like to associate with condensates and higher-twist terms.

Finally, there is a hybrid solution combining the previous types of solutions of Eq. 27 and Eq. 31,

$$G = D_2^{-1/2}; \quad D_2 = t + \frac{3}{4} \ln c_1 t + \dots + 2At^3 e^{-2t} + \dots , \quad (32)$$

where again  $c_1$  and  $A$  are arbitrary. The solutions of the real Schwinger-Dyson equation also ought to have a combination of perturbative powers of logarithms and powers of  $k^2$ . The existence of such hybrid solutions show that more numerical analysis is not very revealing, since it is hard to separate powers and exponentials of  $t$  (i.e., of  $\ln k^2$ ).

An interesting way of looking at our models is to introduce the Laplace transform of  $G(t)$ :

$$G(t) \equiv \int_0^\infty d\alpha F(\alpha) e^{-\alpha t} . \quad (33)$$

Since in the lowest order of approximation  $t \sim (b\bar{g}^2)^{-1}$ , the Laplace transform  $F(\alpha)$  can also be interpreted as the Borel transform. At this order this appears to be a trivial matter, since  $G = b^{1/2}\bar{g}$ ,  $t = (b\bar{g}^2)^{-1}$  leads to  $F(\alpha) = (\pi\alpha)^{-1/2}$ . But as one goes on more interesting phenomena appear.

By recognizing  $e^{-\alpha t} = (k^2/\mu^2)^{-\alpha}$  and using standard integration formulas, one can express the massless integral equation Eq. 23 in the form

$$F(\alpha) = \frac{\alpha}{2-\alpha} \int [dy] F(\alpha y_1) F(\alpha y_2) F(\alpha y_3) \quad (34)$$

where  $[dy] \equiv \int_0^1 dy_1 dy_2 dy_3 \delta(1 - \sum y_i)$ . Here  $y_i$  are Feynman parameters used to express the Laplace transform variables ( $\alpha_i = \alpha y_i$ ) of the three vertices on the right hand side of Eq. 23. Perturbation theory corresponds to  $\alpha \ll 1$ , in which instance we replace  $2 - \alpha$  by 2, and verify that  $F = (\pi\alpha)^{-1/2}$  (i.e.,  $G = t^{-1/2}$ ) is the small- $\alpha$  solution. But there clearly is some sort of singularity at  $\alpha = 2$ , which actually causes Eq. 22 to be meaningless (just as integrals leading to IR renormalons are meaningless). Consider the “approximation” of replacing the  $F(\alpha y_i)$  by their perturbative values on the right hand side of Eq. 34; the result is an  $F(\alpha)$  behaving like  $\alpha^{-1/2}/(2 - \alpha)$ . We can then construct the Laplace transform for  $\beta(\bar{g}) \sim \dot{G}$ , and in  $e^{-\alpha t}$  replace  $t$  by  $(b\bar{g}^2)^{-1}$ . The result is a Borel-transform representation of  $\beta(g)$ ,

$$\beta(g) \sim \int_0^\infty d\alpha \frac{\alpha^{1/2}}{2-\alpha} e^{-\alpha/bg^2} . \quad (35)$$

The pole at  $\alpha = 2$  is, of course, what gives rise to the factorially-divergent behavior of  $\beta$  shown in Eq. 30.

A major theme of our work is the demonstration of how such Borel-transform singularities are cured in the massive theory, as we know they must be. So now we turn to massive models.

## B. Massive Models.

We now return to the massive equation Eq. 22. If  $m \neq 0$  it is no longer possible to find a local differential equation as we did for the massless case, and analytic progress beyond the leading UV behavior seems impossible. However, when  $m = 0$  we can convert Eq. 22 to a differential equation (or a corresponding integral equation in one variable) just as we did when both  $M$  and  $m$  were set to zero. As long as  $M \neq 0$ , there is no IR singularity in Eq. 22, as one easily checks by looking at  $k = 0$ . We will, using the Laplace transform technique, translate this lack of IR divergence into a cancellation mechanism for the poles of the Laplace-transform kernel which appeared in the massless case (see Eq. 34).

We have actually looked at several variants of Eq. 22, which differ in the choice of  $m$  and of the arguments of the  $G$ 's under the integral. These are conveniently summarized via:

$$G(2k^2) = \int \frac{d^6 p}{\pi^3} \frac{F(p, k)}{((p+k)^2 + m^2)^2 (p^2 + M^2)}. \quad (36)$$

The models we will discuss are, for  $M \neq 0$  :

A)  $m = 0$ ,  $F = G^3(2p^2)$  .

B)  $m = M$ ,  $F = G^3(2p^2)$  .

C)  $m = M$ ,  $F = G(2(p+k)^2) G^2(p^2 + k^2 + (p+k)^2)$ .

The  $k$ -independence of  $F$  in models A and B gives rise to one-dimensional integral equations which we analyze both analytically and numerically. Model C, on the other hand, is Eq. 22 with  $m = M$  which gives rise to a two-dimensional integral equation which we attack numerically. In addition to models A-C we have also examined intermediate cases where, for example,  $F = G^3(2(p+k)^2)$  with  $m = M$  or  $F = G^3(2(p^2 + k^2))$  with  $m = M$ . These additional cases introduce a  $k$ -dependence into  $F$  which is still mild enough to yield one-dimensional integral equations. However, since these additional models have all the same qualitative features as models A-C but yield little extra insight, we will not discuss them further.

Only model A will be discussed in much detail. One can show that all models lead to the same leading UV behavior ( $G \rightarrow (\ln k^2)^{-1/2}$ ), and numerical work displayed later shows that the models

differ quantitatively but not qualitatively in the IR. All have the curious feature, mentioned in Section I, that the solutions to each model depend on a single real parameter.

Consider now model A. Similar to our treatment of the massless model, we introduce the variables

$$t = \ln\left(\frac{k^2 + M^2}{M^2}\right), \quad t' = \ln\left(\frac{p^2 + M^2}{M^2}\right) \quad (37)$$

where we have fixed the analog of the arbitrary mass scale  $\mu$  in Eq. 24 to be equal to  $M$ . In terms of these variables, Eq. 36 for model A reads

$$G(t) = \frac{1}{2} \int_0^\infty dt' G^3(t') + \frac{1}{2} \int_0^t dt' \left[ \left( \frac{e^{t'} - 1}{e^t - 1} \right)^2 - 1 \right] G^3(t') . \quad (38)$$

which is equivalent to the differential equation

$$(1 - e^{-t})\ddot{G} + (2 + e^{-t})\dot{G} = -G^3 \quad (39)$$

with the boundary conditions

$$G(0) = \frac{1}{2} \int_0^\infty dt' G^3(t'), \quad G(\infty) = 0 . \quad (40)$$

This differential equation differs from the massless equation Eq. 26 by the appearance of  $e^{-t}$  in the coefficients; it can, of course, be derived directly from Eq. 38, just as we did for the massless equation Eq. 26.

It is not hard to see that  $G(\infty) = 0$  is not really a boundary condition since all solutions of Eq. 39 vanish at  $t = \infty$ . Moreover, Eq. 40 does not constrain  $G(0)$ ; as long as  $G(0) > 0$ , there is a solution to Eq. 39 satisfying Eq. 40. So  $G(0)$  itself can be chosen as the parameter of the solution. Once  $G(0)$  is picked, the solution is unique. All of the models listed above have this feature.

To see how this parameter arises for Eq. 38, consider a slightly different equation with an explicit parameter  $a$ :

$$\tilde{G}(t, a) = a - \frac{1}{2} \int_0^t dt' \tilde{G}(t', a)^3 + \frac{1}{2} \int_0^t dt' \left( \frac{e^{t'} - 1}{e^t - 1} \right)^2 \tilde{G}(t', a)^3 . \quad (41)$$

For  $t \gg 1$  the factor  $(e^{t'} - 1)^2 / (e^t - 1)^2$  is exponentially peaked at  $t' = t$  so it is a good approximation to evaluate the relatively slowly varying  $\tilde{G}(t', a)^3$  at  $t' = t$  and pull it outside the integral to get

$$\tilde{G}(t \gg 1, a) = a - \frac{1}{2} \int_0^{t \gg 1} dt' G(t', a)^3 + \frac{1}{8} \tilde{G}(t \gg 1, a)^3 . \quad (42)$$

If we use the fact that  $\tilde{G}(t \gg 1, a) \sim 1\sqrt{t}$  and let  $t$  go to infinity, we find

$$a = \frac{1}{2} \int_0^\infty dt' \tilde{G}(t', a)^3 . \quad (43)$$

In other words, if  $\tilde{G}(t, a)$  is a solution to Eq. 41 then  $G(t, a)$  automatically satisfies Eq. 38.

We do not know how to solve Eq. 39 analytically, so yet another presentation of its contents is needed to understand the taming of IR renormalons. We proceed as in the massless case by introducing the Laplace transform Eq. 33, with  $t$  given by Eq. 37. Introducing a Feynman parameter  $x$  for the  $p^2 + M^2$  propagator and performing the momentum-space integral, one gets

$$G(t) = \int_0^\infty d\alpha \alpha \int [dy] F(\alpha y_1) F(\alpha y_2) F(\alpha y_3) \int_0^1 dx \frac{x}{(1 + x(e^t - 1))^\alpha} . \quad (44)$$

The  $x$ -integral is elementary, and gives:

$$G(t) = \int d\alpha \alpha \int [dy] \frac{F(\alpha y_1) F(\alpha y_2) F(\alpha y_3)}{(1 - e^{-t})^2} \left( \frac{1}{2 - \alpha} (e^{-\alpha t} - e^{-2t}) - \frac{1}{1 - \alpha} (e^{-(\alpha+1)t} - e^{-2t}) \right) . \quad (45)$$

This is essentially the massive version of Eq. 34 for  $F(\alpha)$ , which is singular at  $\alpha = 2$ . But there is no singularity in the integrand of Eq. 45 for any positive  $\alpha$ . We now see the qualitative (even though quantitatively inaccurate) solution to the IR renormalon problem, expressed as the cancellation by what amounts to condensate terms of poles in the Laplace transform. It is evident that the same sort of cancellation takes place in the  $\beta$ -function, replacing  $e^{-\alpha/bg^2} - e^{-2/bg^2}$  (and, given Eq. 45, another term is added involving a cancelled pole at  $\alpha = 1$ ).

Note, by the way, that it is elementary to derive the differential equation Eq. 39 from Eq. 45: Just form

$$\frac{d}{dt} \left( \frac{e^{-t}}{e^t - 1} \frac{d}{dt} ((e^t - 1)^2 G) \right) . \quad (46)$$

One can look for solutions in the IR or UV by the same method as for the massless equation. There are always well-behaved power-series solutions in  $t$ , with  $G(0)$  as an undetermined parameter; these are useful in the IR. In the UV, there is the same solution in powers of  $t^{-1/2}$  (modulo

logarithms) as for the massless case Eq. 27, but with exponential corrections. There is also an exponentially-vanishing solution based on treating the  $-G^3$  term as a perturbation; the leading term is  $(e^t - 1)^{-2}$  (cf. the massless case Eq. 31). But it appears from numerical studies that this exponentially vanishing solution develops a singularity for some  $t \geq 0$ , which we exclude. Thus the only possibility is the usual UV solution of Eq. 27, at least for generic values of the vertex momenta  $k_i$ .

It might happen that  $\phi_6^3$  has a bound state with the quantum numbers of the  $\phi$ -field, for some particular value of  $k_1^2 \neq 0$ . In that case, the Schwinger-Dyson equation for the bound-state wave function might decrease exponentially in the UV; we have not studied this possibility in detail.

### C. Numerical Solutions.

We have used numerical techniques to solve the integral equations associated with the three models A-C discussed above. Of these only model C gives rise to a two-dimensional integral equation; the others can be put in the one-dimensional form

$$G(t) = \int_0^\infty dt' K(t, t') G^3(t') \quad (47)$$

with different kernels  $K$ . To solve Eq. 47, we put it in the form

$$G(t) = a + \int_0^\infty dt' \tilde{K}(t, t') G^3(t') \quad (48)$$

where  $\tilde{K} = K - 1/2$  and we treat  $a$  as a free parameter, as in Eq. 41. For all kernels,  $\tilde{K}$  falls off rapidly when  $t \gg t'$  and one shows  $a = \frac{1}{2} \int_0^\infty dt G^3$ , as before. The two dimensional integral equation associated with model C is treated in a completely analogous manner, with a similar definition of  $a$ . We have explored thoroughly the range  $0 < a \leq 2$ , and we will show results for  $a = 1, 2$ . All results were calculated to 16 digits precision. For  $a > 2$  it takes progressively longer for our numerical routines to converge so we cannot exclude the possibility of an upper bound to  $a$  above which solutions cease to exist.

Fig. 8 compares models A ( $m = 0$ ) and B ( $m = M$ ). For model B  $G(0) = a$  (see Eq. 40) which is larger than  $G(0)$  for model A, increasingly so as  $a$  gets larger. This comparison shows the effects of varying mass assignments.

Fig. 9 compares models B and C. which have all masses set to the same non-zero value but differ in the arguments of the  $G$ 's in the Schwinger-Dyson equation. For the same  $a$  value (1 in this case) the differences are remarkably small throughout the entire range of momenta. Results such as these give us confidence that toy models, such as model A and B which can be studied analytically to some extent are likely to be representative of the full Schwinger-Dyson equation, even at zero momenta.

The next question to ask is what happens when one goes beyond the cubic term in the Schwinger-Dyson equation.

#### IV. AN APPROACH TO SCHWINGER-DYSON VERTEX GRAPHS OF ALL ORDERS

In this section we take the first incomplete steps towards an analysis of graphs of all orders in the Schwinger-Dyson equation for  $\bar{g}$  or for the proper vertex  $\Gamma$ . These Schwinger-Dyson graphs are expressed by writing all perturbative vertex graphs which have no vertex or self-energy insertions; a few such graphs are shown in Fig. 6. Then in the full Schwinger-Dyson equation each such graph is replaced by one of the same topology but with full vertices and propagators. In what follows we do not need to consider the cubic graph which was the concern of previous sections.

All remaining vertex skeleton graphs have the property that the minimum number of lines in any closed loop is at least four; graph theorists say that such graphs have girth four. It turns out that such bare skeleton graphs, in perturbative  $\phi_6^3$ , have exactly one UV logarithm ( $\ln \Lambda_{\text{UV}}^2$ , where  $\Lambda_{\text{UV}}$  is a UV cutoff) and no IR logarithm ( $\ln M^2$ ). This follows straightforwardly from an elementary remark about  $\phi_4^4$  graphs, as we now show.

Every perturbative skeleton graph of  $N$  loops, ( $3N$  lines,  $2N + 1$  vertices) has the following Feynman-parameter form in Minkowski space, which is for the moment convenient:

$$\Gamma_N^0 = \text{constant} \times g^{2N} \int \frac{[dx]}{U^3} \ln \left( \frac{-\phi/U + \sum x_i M_i^2 - i\epsilon}{\Lambda_{\text{UV}}^2} \right) \quad (49)$$

where  $[dx] = \delta(1 - \sum x_i) \prod_{i=1}^{3N} dx_i$ .  $U$  is the graph's determinant (a positive sum of monomials of order  $N$  in the  $x_i$ ), and  $\phi$  (not to be confused with the field  $\phi$ ) is a sum of positive polynomials in the  $x_i$  times scalar momentum functions  $k_a \cdot k_b$ . The single UV divergence is explicit, and can be

removed by taking the imaginary part of  $\Gamma_N^0$ , replacing the logarithm by a  $\theta$ -function. Any other divergences in the imaginary part must come from the vanishing of  $U$ . But, as is well known,  $U$  can vanish only when at least all the parameters of a loop in the graph go to zero. Let  $\{x_i\}$  be the parameters of one and only one such loop of  $n$  lines, and replace  $x_i$  by  $\lambda x_i$ ,  $\lambda \rightarrow 0$ . Then  $U$  vanishes like  $\lambda$ . But  $[dx]$  behaves like  $\lambda^{n-1} d\lambda$  times irrelevant factors, and the integral is finite if  $n \geq 4$ , that is, for girth-four graphs. If all the parameters of two complete (possibly overlapping loops) are scaled with parameters  $\lambda_1, \lambda_2$ , then  $U$  vanishes like  $\lambda_1 \lambda_2$ , and the argument can be repeated, with some necessary variations. The reader may easily check that only for skeleton graphs the total number of distinct lines in  $\ell$  complete loops is at least  $3\ell + 1$  for any skeleton graph of order  $N > \ell$ . Then the one-loop scaling argument given above can be repeated, and one shows there are no singularities in the Feynman parameter integral. (The case  $N = \ell$  is trivial, since not all the  $x_i$  can be scaled to zero.)

The Minkowski-space imaginary part of  $\Gamma_N^0$  in Eq. 49 is, when all masses are equal to  $M$ ,

$$\text{Im}\Gamma_N^0 = \text{constant} \times g^{2N} \int \frac{[dx]}{U^3} \theta\left(\frac{\phi}{U} - M^2\right). \quad (50)$$

Consider now the kinematics of Fig. 1 where  $k_1, -k_2$ , and  $-k_3$  are forward timelike, with  $k_1^2 = s > 4M^2$ ,  $k_2^2 = k_3^2 = M^2$ . One easily shows  $k_1 \cdot k_2 = k_1 \cdot k_3 = s/2$ ,  $k_2 \cdot k_3 = s/2 - M^2$ , which is enough to show that the argument of the  $\theta$ -function is positive (trivially so at  $M = 0$ ) and thus the  $\theta$ -function can be replaced by unity. We then reduce the problem of finding  $\text{Im}\Gamma_N^0$  to summing the integrals

$$\int \frac{[dx]}{U_i^3} \quad (51)$$

where  $i$  runs over all the  $N$ -th order skeleton graphs. This problem (with  $U_i^{-3} \rightarrow U_i^{-2}$ ) has been addressed for  $\phi_4^4$  [7], using the following steps which we will repeat here.

1. Count all the  $N^{\text{th}}$  order graphs, and note that the number of these which are not skeleton graphs vanishes at large  $N$  relative to the number of skeleton graphs. We denote this number as  $Q_N$ .

2. Find, by a combination of analysis and numerical work, the number  $C_i$  of monomials in  $U_i$ . This number is called the complexity of the graph, and is equal to the number of spanning trees.

3. Show that

$$\langle U \rangle_i \equiv \frac{\int [dx] U_i}{\int [dx]} = C_i \frac{(3N-1)!}{(4N-1)!} . \quad (52)$$

That is, every monomial in  $U_i$  contributes exactly the same to  $\langle U \rangle_i$ .

4. Use a Hölder inequality to show

$$\left\langle \frac{1}{U} \right\rangle_i^3 \geq \frac{1}{\langle U \rangle_i^3} . \quad (53)$$

5. Observe that the distribution of  $C_i$  for all the  $N$ -loop graphs centers around an average value  $\langle C \rangle$ .

We then have, inserting the usual powers of  $2\pi$ ,

$$\text{Im} \Gamma_N^o \gtrsim \left( \frac{g^2}{(4\pi)^3} \right)^N Q_N \frac{1}{\langle U \rangle_i^3} . \quad (54)$$

Now Bender and Canfield [14] have shown, in a deep graph-theoretic result, that

$$Q_N \doteq \left( \frac{3}{2} \right)^N N! \quad (55)$$

and we have made a numerical analysis of large- $N$  graphs to find

$$\langle C \rangle \doteq \left( \frac{16}{3} \right)^N . \quad (56)$$

(Here  $A_N \doteq B_N$  if  $A_N, B_N$  are each of the form  $c_o(N!)^{c_1} c_2^N N^{c_3} (1 + O(1/N))$  at large  $N$ , and the constants  $c_1$  and  $c_2$  are the same for  $A_N$  and  $B_N$ .)

Putting everything together,

$$\text{Im} \Gamma_N^o \geq N! \left[ \frac{a g^2}{(4\pi)^3} \right]^N , \quad a = \frac{2^{11}}{3^8} \simeq 0.312 . \quad (57)$$

As expected for an asymptotically free theory, this is not Borel-summable.

Even though extracted from a high-energy process in Minkowski space, the result of Eq. 57 looks exactly like what one would expect from a lowest-order (semi-classical) instanton calculation which requires zero external momenta and masses. There is no sign of external momenta or masses in Eq. 57, which renders this formula compatible with the Lipatov procedure. So let us compare the coefficient  $a$  in Eq. 57 to the instanton result. As is well known [5], there are instantons in massless  $\phi_6^3$ , of the form

$$\phi_{c\ell} = \frac{48\rho^2}{g[(x-a)^2 + \rho^2]^2} \quad (58)$$

whose action is

$$I = \left(\frac{12}{5}\right) \frac{(4\pi)^3}{g^2} . \quad (59)$$

This means that using the Lipatov procedure one would find an expression of the form of Eq. 57 for  $\text{Im}\Gamma_N^o$ , with  $a = 5/12 = 0.417$ . Our lower-limit value  $2^{11}/3^8$  is about 3/4 of this (presumably correct) value, and further numerical work, which we have not done, would bring this lower-limit value closer to the true value of  $a$ .

The fact that there are no logarithms in  $\text{Im}\Gamma_N^o$  (or only one in  $\Gamma_N^o$ ) is of vital importance for analyzing the Schwinger-Dyson equation, when full propagators and vertices are used to dress the bare skeleton graph. This amounts to inserting  $2N + 1$  factors of  $\bar{g}$  (see Eq. 19), where every  $\bar{g}$  behaves like  $(b \ln k^2)^{-1/2}$  for the appropriate momentum  $k$ . One should then not be surprised to find that the  $N$ -loop full skeleton graphs behave, for large external momentum  $k$ , like  $(\ln k^2)^{-\frac{1}{2}(2N+1)+1}$  and that the sum of full skeleton graphs is of the form Eq. 57, with  $g^2$  replaced by the (one-loop) running charge  $\bar{g}^2$ . The Schwinger-Dyson equation thus yields the results of RG-improved instanton calculations, with no explicit introduction of instantons.

We will not show the derivation of this result in detail, but merely sketch it. As in Section III we make the approximation that every  $\bar{g}$  depends only on  $\sum k_i^2$ , where  $k_i$  are the vertex momenta, and introduce the Laplace transform

$$\bar{g}(k_i) = \int d\alpha F(\alpha) e^{-\alpha \ln(\sum k_i^2)} . \quad (60)$$

Anticipating that the leading UV behavior of the  $N^{\text{th}}$  order graphs is dominated by the UV behavior of the cubic graph studied in Section 3, we choose

$$F(\alpha) = (\pi b \alpha)^{-1/2} \quad (61)$$

corresponding to  $\bar{g} \rightarrow (b \ln k^2)^{-1/2}$ .

As before, the factor  $\exp(-\alpha \ln \sum k_i^2)$  is written as  $(\sum k_i^2)^{-\alpha}$  and the momentum integrals are done after Feynman parameterization. A tedious analysis, not given here, shows that one need not

introduce  $2N + 1$  new Feynman parameters for the new denominators  $\sum k_i^2$ ; instead, one shows that the correct asymptotic behavior is also found by replacing such denominators by those of neighboring propagators. The result is that many of the propagators in a bare skeleton graph appear to powers  $-(1 + \alpha_i)$ , where  $\alpha_i$  is the Laplace transform variable of a neighboring vertex. Finally one finds, setting the mass  $M$  to zero, and going to asymptotically-large  $k$  as in Section 3,

$$\bar{g}_N = Q_N \left[ \frac{1}{\pi(4\pi)^3 b} \right]^N \int \Pi \alpha_i^{-1/2} d\alpha_i \Gamma(\sum \alpha_i) [\Pi \Gamma(1 + \alpha_i)]^{-1} \int \frac{[dx]}{U^3} \Pi x_i^{\alpha_i} \left( \frac{\phi}{k^2 U} \right)^{-\sum \alpha_i} \quad (62)$$

where  $\phi$  and  $U$  are the appropriate functions for the bare skeleton graph, and an irrelevant constant factor has been dropped. In the result of Eq. 61,  $Q_N$  is the number of  $N^{\text{th}}$ -order skeleton graphs, given in Eq. 55.

In the kinematics of Fig. 7,  $\phi$  is of the form of  $k^2$  times a function of  $y_i$ . We scale the  $\alpha_i$  by  $\alpha_i = \alpha y_i$ , with  $\sum y_i = 1$ , and get

$$\bar{g}_N = \int_0^\infty d\alpha \frac{\alpha^{N-\frac{3}{2}}}{\Gamma(N-\frac{1}{2})} e^{-\alpha \ln k^2} H(\alpha) \quad (63)$$

where

$$H(\alpha) = \Gamma(N - \frac{1}{2}) \left[ \frac{1}{\pi(4\pi)^3 b} \right]^N Q_N \int [dy] \Pi y_i^{-1/2} \Gamma(1 + \alpha) \int \frac{[dx]}{U^3} \Pi x_i^{\alpha_i} \left( \frac{\phi}{k^2 U} \right)^{-\alpha}. \quad (64)$$

In Eq. 63 and Eq. 64 we wrote  $\Gamma(\sum \alpha_i) \equiv \Gamma(\alpha)$  as  $\alpha^{-1} \Gamma(1 + \alpha)$  and removed a factor  $\Gamma(N - \frac{1}{2})$  for simplicity. This allows us to assert that  $H(\alpha)$  is regular at  $\alpha = 0$ , and in fact one checks easily that

$$H(0) \doteq \left[ \frac{1}{\pi(4\pi)^3 b} \right]^N Q_N \int \frac{[dx]}{U^3} \quad (65)$$

which is just the function appearing in the sum of bare skeleton graphs. It is clear from Eq. 63 that the leading asymptotic behavior of  $\bar{g}_N$  comes from  $\alpha \simeq 0$ , which gives

$$\bar{g}_N \doteq H(0) \int d\alpha \frac{\alpha^{N-\frac{3}{2}}}{\Gamma(N-\frac{1}{2})} e^{-\alpha \ln k^2} \doteq N! \left[ \frac{a}{(4\pi)^3 b \ln k^2} \right]^N \quad (66)$$

using the previous result for  $H(0)$ .

This is as far as we will carry the analysis. We have no particularly good ideas for extending the toy models of Section III to all orders in a controllable way. Nor will we attempt to find some

physical way to sum the series of Eq. 66 (based, e.g., on decay of the meta-stable vacuum). If the sum of terms is represented by a (formal) Borel transform, there arises an ambiguity of the form  $(k^2)^{-c}$ , where  $c = (4\pi)^3 b/a$ . This is of the usual type associated with RG-improved instantons.

## V. CONCLUSIONS

In the long run, perturbative QCD must fail because of its IR singularities, and some sort of new perturbative analysis of Schwinger-Dyson equations will have to be seriously attempted. This is much more difficult than  $\phi_6^3$ , because of the complications of spin, gauge dependence, and confinement. Still, we believe that some of our results will hold for QCD, in particular, the cancellation of poles in Borel transforms as in Eq. 2. Currently there is considerable phenomenological interest [2] in renormalon problems, and it would be valuable to test the mechanism we identify as relevant, versus other prescriptions such as principal part integration.

A similar mechanism may well hold for Borel transforms associated with instantons, although we are unable to say in  $\phi_6^3$  because of its instability. In QCD (or a similarly-stable asymptotically free theory, like the  $d = 2$  nonlinear  $\sigma$  model), it is quite important to learn how to deal with phenomena canonically associated with instantons (e.g., the Lipatov technique) by other means than the usual RG-corrected semi-classical results, because the perturbative corrections to semi-classical instanton physics involve IR singularities such as renormalons. Understanding such phenomena directly from the Schwinger-Dyson equations is a worthwhile thing to do. Moreover, at the moment Schwinger-Dyson equations are the most straightforward way of dealing [7] with the non-Borel-summable divergences at large Minkowski-space external momenta. We hope to report in the future on future progress in this direction, going well beyond the first steps of Section IV.

We have seen that all the toy models of the Schwinger-Dyson equation have solutions with a free parameter, equivalent to the renormalization mass  $\mu$ . Since  $\mu$  comes in as a tool in dealing with amplitudes needing regularization, and since asymptotically free Schwinger-Dyson equations in their canonical form need no such regularization, this is a bit of a surprise. On the other hand, one would be surprised if a single Schwinger-Dyson equation—in our case, that for the running charge defined in Eq. 19—had a single solution for the three-point function, making no reference

to higher-point functions as the usual hierarchy argument specifies. It remains to be seen how this is settled by consideration of further Schwinger-Dyson equations.

## **VI. ACKNOWLEDGMENTS**

One of us (JMC) was supported in part by NSF Grant PHY-9218990. Both of us thank J. Ralston and W. Newman for useful conversations.

## REFERENCES

- [1] G. 't Hooft, in *The Whys of Subnuclear Physics*, Proceedings of the 15<sup>th</sup> International School on Subnuclear Physics, Erice, 1977, edited by A. Zichichi (Plenum Press, New York, 1979), p. 943.
- [2] V.I. Zakharov, Nucl. Phys. **B385**, 452 (1992); C.N. Lovett-Turner and C.J. Maxwell, Durham preprint DTP/95/36, April 1995 (unpublished); A. Duncan and S. Pernice, Phys. Rev. D **51**, 1956 (1995); M. Neubert, Phys. Rev. D **51**, 5924, (1995).
- [3] For perturbative RG calculations, see A.J. MacFarlane and G. Woo, Nucl. Phys. **B77**, 91 (1974); J.C. Collins, *Renormalization*, (Cambridge University Press, Cambridge, 1984).
- [4] A previous study (J. M. Cornwall and J. Papavassiliou, Phys. Rev. D **40**, 3479 (1989)) studied equations similar to those of the present paper for a very simplified model of d=4 QCD.
- [5] A. J. Houghton, J. S. Reeve, and D. J. Wallace, Phys. Rev. B **17**, 2956 (1978).
- [6] The instanton techniques for finding  $N!$  terms is due to L. N. Lipatov, Pis'ma Zh. Eksp. Teor. Fiz. **24**, 179 (1976) [JETP Lett. **24**, 157 (1976)], and was implemented in detail by E. Brézin, J. C. le Guillou, and J. Zinn-Justin, Phys. Rev. D **15**, 1544 (1977); **15**, 1558 (1977). For other references, see *Large-Order Behavior of Perturbation Theory*, edited by J. C. le Guillou, and J. Zinn-Justin, Current Physics Sources and Comments Vol. 7 (North-Holland, Amsterdam, 1990).
- [7] J. M. Cornwall and D.A. Morris, Phys. Rev. D **51**, 4894 (1995).
- [8] J. M. Cornwall and G. Tiktopoulos, Phys. Rev. D **45**, 2105 (1992).
- [9] J. M. Cornwall, Phys. Rev. D **26**, 1453 (1982).
- [10] There are general arguments why some such removal of imaginary parts must occur; see E. Bogomol'nyi, Phys. Lett. B **91**, 431 (1980); J. Zinn-Justin, Nucl. Phys. B **192**, 125 (1981); V. I. Zakharov, Nucl. Phys. B **377**, 501 (1992). Sometimes the closely-

related principal-part regularization of integrals like (1.1) is used for phenomenology; see H. Contopanagos and G. Sterman, Nucl. Phys. B**419**, 77 (1994).

[11] In the Yang-Lee edge for ferromagnets, see M. E. Fisher, Phys. Rev. Lett. **40**, 1610 (1978).

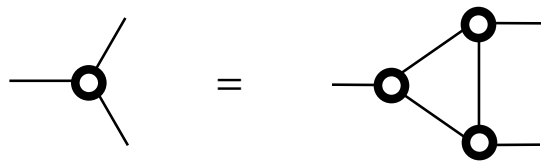
[12] In Reggeon field theory, see H. Abarbanel, J. Bronzan, R. Sugar, and A. White, Phys. Rep. **21C**, 119 (1975).

[13] N. Nakanishi, Prog. Theor. Phys. (Kyoto) **23**, 1151 (1960).

[14] E. A. Bender and E. R. Canfield, J. Comb. Theory A**24**, 296 (1978).

## FIGURE CAPTIONS

1. Bethe-Salpeter equation for the renormalized three-point function (small blobs) expressed in terms of the two-particle-irreducible (in the  $k_1$  channel) four-point function (large blob) and the vertex renormalization constant  $Z_1$ . All propagators are fully dressed.
2. Bethe-Salpeter equation for the renormalized three-point function (small blobs) expressed in terms of the one-particle-irreducible (in the  $k_1$  channel) four-point function (large blob) and the vertex renormalization constant  $Z_1$ . All propagators are fully dressed.
3. Bethe-Salpeter equation for the renormalized inverse propagator in terms of the renormalized three-point-function and the vertex renormalization constant  $Z_1$ . All propagators are fully dressed.
4. Lowest order approximations to the Schwinger-Dyson equations for a) the three point function and b) the inverse propagator.
5. Cubic Schwinger-Dyson equation in  $g|\psi|^2\phi$  theory.
6. Schwinger-Dyson equation for the running charge (solid blob). All propagator lines are free propagators with renormalized masses.
7. Momentum assignments for the truncated Schwinger-Dyson equation for the running charge.
8. Numerical solutions of the toy-model Schwinger-Dyson equation for models A and B for  $a = 1, 2$  where  $a = 1/2 \int dt' G^3(t')$ .
9. Numerical solutions of the toy-model Schwinger-Dyson equation for models B and C for  $a = 1$ .



(a)

$$\Delta^{-1} = \Delta_0^{-1} + \text{diagram with two vertices and a loop}$$

(b)

Fig. 4

$$\text{wavy line} \circ \gamma = \text{wavy line} \text{ with slash } Z_2 + \text{wavy line} \circ \gamma \text{ with loop} + \dots$$

Fig. 5

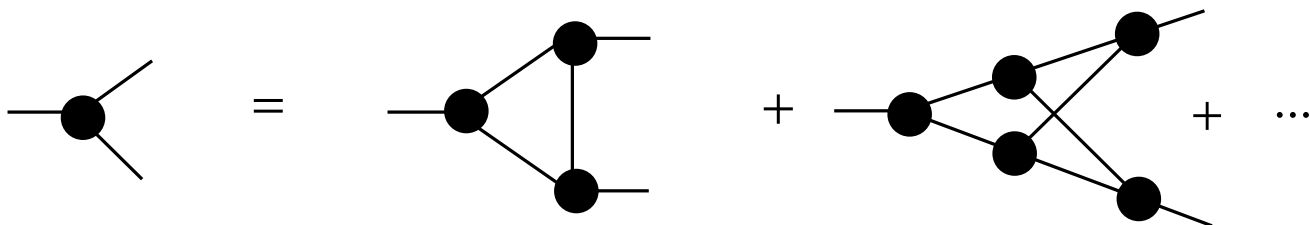


Fig. 6

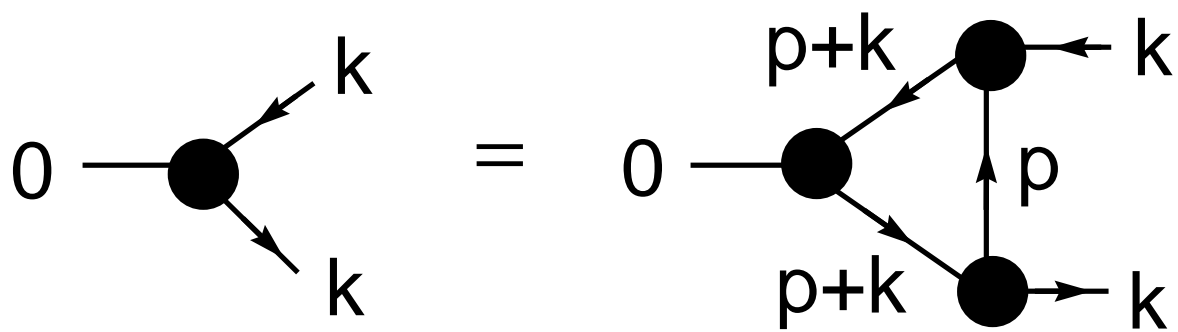


Fig. 7

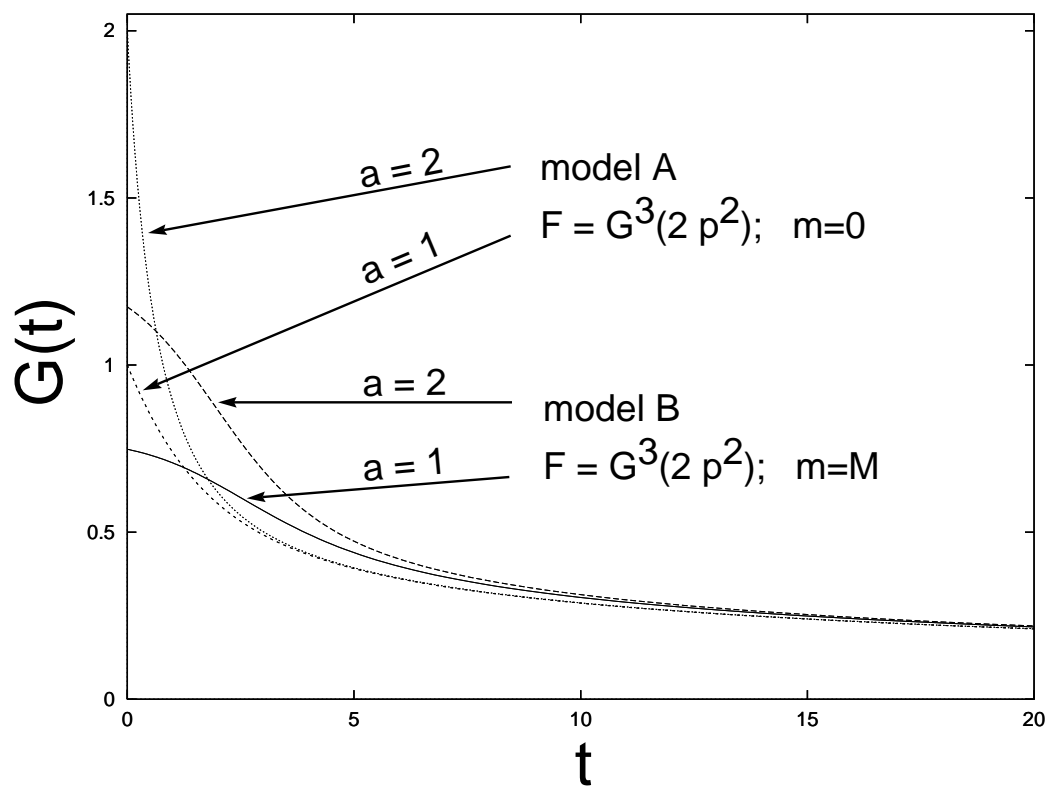


Fig. 8

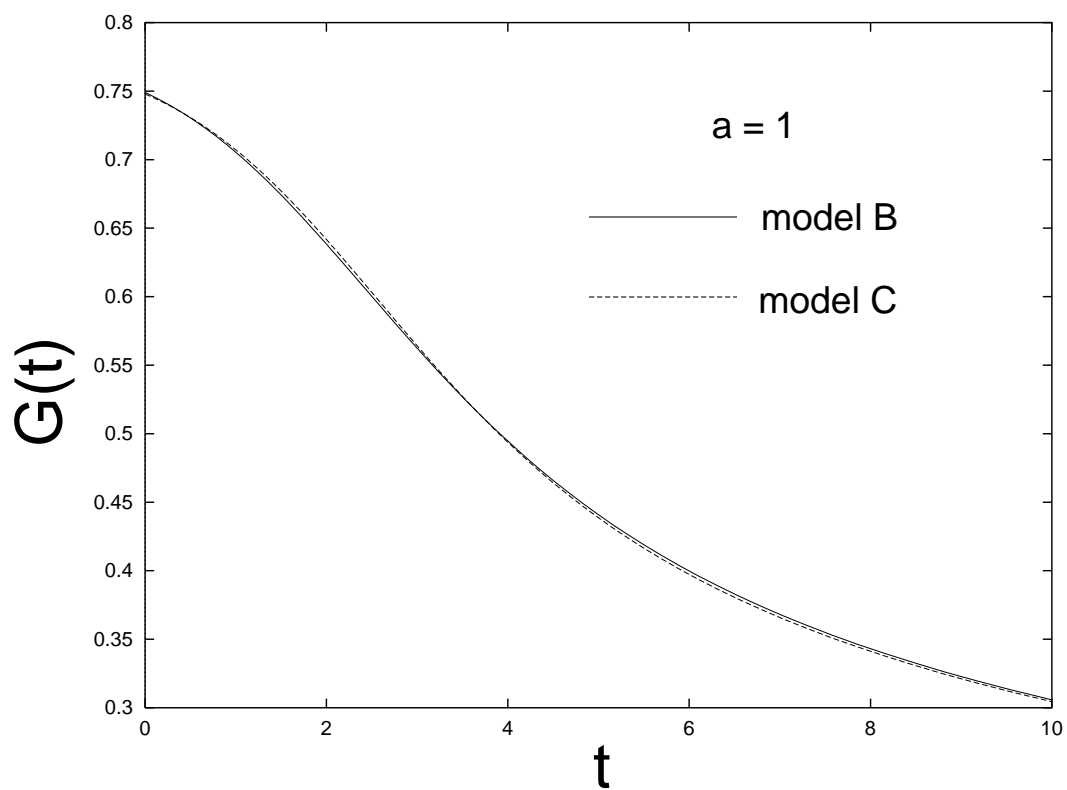


Fig. 9

$$\begin{aligned}
 \Gamma &= \begin{array}{c} k_2 \\ \nearrow \\ k_1 \rightarrow \bullet \\ \searrow \\ k_3 \end{array} \\
 &= Z_1 + \text{---} \bullet \text{---} \bigcirc \text{---} \text{---} \quad (2) \\
 &= Z_1 + \text{---} \bullet \text{---} \begin{array}{c} \circ \\ \diagup \quad \diagdown \\ \circ \end{array} \text{---} \text{---} + \text{---} \bullet \text{---} \begin{array}{c} \circ \quad \circ \\ \diagup \quad \diagdown \quad \diagup \quad \diagdown \\ \circ \quad \circ \end{array} \text{---} \text{---} + \dots
 \end{aligned}$$

Fig. 1

$$\begin{aligned}
 \Gamma &= Z_1 + Z_1 \text{---} \text{---} \bigcirc \text{---} \text{---} \quad (1) \\
 &= Z_1 + Z_1 \text{---} \begin{array}{c} \circ \\ \diagup \quad \diagdown \\ \circ \end{array} \text{---} \text{---} + Z_1 \text{---} \begin{array}{c} \circ \quad \circ \\ \diagup \quad \diagdown \quad \diagup \quad \diagdown \\ \circ \quad \circ \end{array} \text{---} \text{---} + Z_1 \text{---} \begin{array}{c} \circ \quad \circ \\ \diagup \quad \diagdown \quad \diagup \quad \diagdown \\ \circ \quad \circ \end{array} \text{---} \text{---} + \dots
 \end{aligned}$$

Fig. 2

$$\begin{aligned}
 \Delta^{-1} &= \Delta_0^{-1} + Z_1 \text{---} \text{---} \bigcirc \text{---} \text{---} \\
 &= \Delta_0^{-1} + \text{---} \bigcirc \text{---} \bigcirc \text{---} \text{---} - \text{---} \bigcirc \text{---} \bigcirc \text{---} \text{---} \quad (2)
 \end{aligned}$$

Fig. 3